

Synthesis and Characterization of Iridium 1,3,5-Triaza-7-phosphaadamantane (PTA) Complexes. X-ray Crystal and Molecular Structures of $[\text{Ir}(\text{PTA})_4(\text{CO})]\text{Cl}$ and $[\text{Ir}(\text{PTAH})_3(\text{PTAH}_2)(\text{H})_2]\text{Cl}_6$

Don A. Krogstad,^{*,†} Jason A. Halfen,[‡] Tracy J. Terry,[†] and Victor G. Young, Jr.[§]

Departments of Chemistry, The University of the South, Sewanee, Tennessee 37375,
The University of Wisconsin–Eau Claire, Eau Claire, Wisconsin 54702, and
The University of Minnesota, Minneapolis, Minnesota 55455

Received May 9, 2000

The first 1,3,5-triaza-7-phosphaadamantane (PTA) ligated iridium compounds have been synthesized. The reaction of PTA with $[\text{Ir}(\text{COD})\text{Cl}]_2$ (COD = 1,5-cyclooctadiene) under a CO atmosphere produces an inseparable mixture of $[\text{Ir}(\text{PTA})_3(\text{CO})\text{Cl}]$ (**1**) and the PTA analogue of Vaska's compound, $[\text{Ir}(\text{PTA})_2(\text{CO})\text{Cl}]$ (**2**). Compound **1** and $[\text{Ir}(\text{PTA})_4(\text{CO})]\text{Cl}$ (**3**) were prepared via ligand substitution reactions of PTA with Vaska's compound, *trans*- $\text{Ir}(\text{PPh}_3)_2(\text{CO})\text{Cl}$, in absolute and 95% ethanol, respectively. Complex **3** crystallizes in the orthorhombic space group *Pbca* with $a = 20.3619(4)$ Å, $b = 14.0345(3)$ Å, $c = 24.1575(5)$ Å, and $Z = 8$. Single-crystal X-ray diffraction studies show that **3** has a trigonal bipyramidal structure in which the CO occupies an axial position. This is the first crystallographically characterized $[\text{IrP}_4(\text{CO})]^+$ complex in which the CO is axially ligated. Compound **1** was converted into **3** by ligand substitution with 1 equiv of PTA in water. Interestingly, the reaction of **3** with excess NaCl did not result in the production of **1**, but instead the formation of the dichloro species, $[\text{Ir}(\text{PTAH})_2(\text{PTA})_2\text{Cl}_2]\text{Cl}_3$ (**4**) (PTAH = protonated PTA). Dissolution of **1** or **3** in dilute HCl produced **4** and a dihydrido species, $[\text{Ir}(\text{PTAH})_4(\text{H})_2]\text{Cl}_5$ (**5**), which were readily separated by inspection due to their different crystal habits. Compound **5** crystallizes in the triclinic space group *P* $\bar{1}$ with $a = 12.4432(9)$ Å, $b = 12.5921(9)$ Å, $c = 16.3231(12)$ Å, $\alpha = 76.004(1)^\circ$, $\beta = 71.605(1)^\circ$, $\gamma = 69.177(1)^\circ$, and $Z = 2$. Complex **5** exhibits a distorted octahedral geometry with two hydride ligands in a *cis* configuration. A rationale consistent with these reactions is presented by consideration of the steric and electronic properties of the PTA ligand.

Introduction

Over the past 5 decades, transition metal complexes have found utility as both catalysts and models for catalytic systems.¹ A number of iridium complexes have been extensively studied for these purposes because of their relative stability and ease of characterization. For example, $\text{Ir}(\text{PPh}_3)_3\text{Cl}$, the iridium analogue of Wilkinson's catalyst,² and a similar complex, *trans*- $[\text{Ir}(\text{PPh}_3)_2(\text{CO})\text{Cl}]$, Vaska's compound,³ were thoroughly examined to better understand the oxidative addition of small molecules in organic media. Later, Crabtree observed that the related complexes $[\text{IrL}_2(\text{COD})]\text{PF}_6$ and $[\text{IrL}(\text{COD})(\text{py})]\text{PF}_6$ (COD = 1,5-cyclooctadiene, L = tertiary phosphine, py = pyridine) were very active catalysts for homogeneous hydrogenation.⁴

Homogeneous catalysts, such as $[\text{Ir}(\text{PPh}_3)_2(\text{COD})]\text{PF}_6$ and $[\text{IrL}(\text{COD})(\text{py})]\text{PF}_6$, often possess three characteristics, which limit their utility: (1) difficulty in the separation of the catalyst from the reaction products, (2) difficulty in the recovery of the expensive transition metal catalyst, and (3) exclusive utilization of environmentally hazardous solvents.⁵ One possible way to circumvent these problems has been to use a two-phase process in which a water-soluble catalyst is dissolved and employed in the aqueous phase, while the substrate is immersed in an immiscible organic media. This allows the isolation of metal-free, organic products and intact catalyst by phase separation while using a minimal amount of potentially hazardous solvent.⁵

Because of the environmental and potential industrial importance of aqueous organometallic reactions, water-soluble compounds have recently received a fair amount of attention.⁶ Most compounds in these studies have been prepared by complexation of an appropriate metal with ionic or polar phosphines⁷ such as the monosulfonated (tpms) and the trisulfonated (tppts) derivatives of triphenylphosphine^{5–8} or

* To whom correspondence should be addressed. Present address: Department of Chemistry, Minnesota State University Moorhead, Moorhead, Minnesota, 56563. Telephone: 218-291-4371. Fax: 218-236-2137.

[†] The University of the South.

[‡] The University of Wisconsin–Eau Claire.

[§] The University of Minnesota.

- (1) Collmann, J. P.; Hegedus, L. S.; Norton, J. R.; Finke, R. G. *Principles and Applications of Organotransition Metal Chemistry*; University Science Books: Mill Valley, CA, 1987.
- (2) (a) Collmann, J. P.; Kubota, M.; Vastina, F. D.; Sun, J. Y.; Kang, J. W. *J. Am. Chem. Soc.* **1968**, *90*, 5430. (b) Bennett, M. A.; Milner, D. L. *J. Am. Chem. Soc.* **1969**, *91*, 6983. (c) Bennett, M. A.; Charles, R.; Mitchell, T. R. B. *J. Am. Chem. Soc.* **1978**, *100*, 2739.
- (3) (a) Chock, P. B.; Halpern, J. *J. Am. Chem. Soc.* **1966**, *88*, 3511. (b) Vaska, L. *Acc. Chem. Res.* **1968**, *1*, 335. (c) Collman, J. P. *Acc. Chem. Res.* **1968**, *1*, 136. (d) Ugo, R.; Pasini, A.; Fusi, A.; Cenini, S. *J. Am. Chem. Soc.* **1972**, *94*, 7364.

- (4) (a) Crabtree, R. *Acc. Chem. Res.* **1979**, *12*, 331. (b) Crabtree, R. H.; Felkin, H.; Morris, G. E. *J. Organomet. Chem.* **1977**, *141*, 205. (c) Crabtree, R. H.; Felkin, H.; Morris, G. E. *J. Chem. Soc., Chem. Commun.* **1976**, 716.
- (5) (a) Papadogianakis, G.; Sheldon, R. A. *New J. Chem.* **1996**, *20*, 175. (b) Herrmann, W. A.; Kohlpainter, C. W. *Angew. Chem., Int. Ed. Engl.* **1993**, *32*, 1524.
- (6) Several reviews have been written on this topic. (a) Nomura, K. *J. Mol. Catal. A.* **1998**, *130*, 1. (b) Joo, F.; Katho, A. *J. Mol. Catal. A.* **1997**, *116*, 3. (c) Roundhill, D. M. *Adv. Organomet. Chem.* **1995**, *38*, 155.

1,3,5-triaza-7-phosphaadamantane (PTA).⁹ PTA has a very small cone angle (103°)¹⁰ and is more resistant to oxidation than tppms and tppts. Therefore, recent research has centered on the synthesis of PTA ligated complexes¹¹ and their use as homogeneous and biphasic catalysts.¹² For example, Pruchnik prepared a Rh analogue of Vaska's compound, *trans*-[Rh(PTA)₂(CO)Cl], which catalyzes the reduction of CO₂ with H₂.¹³ Joo et al. demonstrated that an analogue of Wilkinson's catalyst, [Rh(PTA)₃Cl], catalyzes the regioselective reduction of aldehydes¹⁴ and the hydrogenation of olefinic and oxo acids¹⁵ and phospholipid liposomes.¹⁶ Surprisingly, even with the historic modeling and catalytic abilities of iridium phosphine complexes, no one has reported on the study of Ir–PTA complexes.^{10–16} Therefore, we have recently investigated this topic and wish to report on the synthesis and characterization of the first Ir(I)–PTA complexes [Ir(PTA)₃(CO)Cl] (**1**), [Ir(PTA)₂(CO)Cl] (**2**), and [Ir(PTA)₄(CO)]Cl (**3**) and the reactivity of **1** and **3** with aqueous HCl to form the Ir(III)–PTA complexes *cis*-[Ir(PTAH)₂(PTA)₂Cl₂]Cl₃ (**4**) (PTAH = protonated PTA) and *cis*-[Ir(PTAH)₄(H₂)Cl₅] (**5**). Crystals of **5** desolvate and eliminate HCl upon exposure to air. Consequently, samples of varying degrees of ligand protonation have been collected and characterized. Therefore, for the sake of simplicity, compound **5** will be addressed in this manuscript as the tetraprotonated species, [Ir(PTAH)₄(H₂)Cl₅], unless otherwise noted.

Experimental Section

General Procedure, Measurements, and Materials. All manipulations were carried out under a purified N₂ atmosphere with use of standard Schlenk techniques unless otherwise noted. This airless procedure was used even though the final complexes are air stable. Elemental analyses were carried out by Galbraith Laboratories, Inc., Knoxville, TN. Fast atom bombardment mass spectrometric (FAB-MS) experiments were carried out with the use of a VG Analytical, Ltd.,

7070E-HF high-resolution double-focusing mass spectrometer equipped with a VG 11/250 data system. Infrared spectra were measured in KBr pellets on a Perkin–Elmer 1710 FT-IR spectrometer. ³¹P{¹H} and ¹H NMR spectra were recorded at 121.5 and 300 MHz, respectively, with use of a Varian VXR-300 MHz spectrometer. The ³¹P spectra were run with proton decoupling and are reported in ppm relative to an external H₃PO₄ standard, with positive shifts downfield. Solvents were distilled and dried prior to use. CO was obtained from Aldrich and used without further purification. 1,3,5-triaza-7-phosphaadamantane (PTA), *trans*-[Ir(PPh₃)₂(CO)Cl], and [Ir(COD)Cl]₂ (COD = 1,5-cyclooctadiene) were prepared as described in the literature.^{17,18,19}

Preparation of Complexes. [Ir(PTA)₃(CO)Cl] (1**). Method A.** A 100-mL Schlenk flask was charged with a 52.5-mg (0.0673-mmol) sample of *trans*-[Ir(PPh₃)₂(CO)Cl], a 63.5-mg (0.404 mmol) sample of PTA, and 30 mL of absolute ethanol to form a greenish yellow slurry. The slurry was heated to reflux and allowed to stir for 12 h. Upon cooling to room temperature, the resulting pale yellow-green precipitate was collected on a medium frit under N₂, washed with benzene (3 × 10 mL), chloroform (3 × 10 mL), and diethyl ether (3 × 10 mL), and dried in vacuo (yield: 37.8 mg, 0.0520 mmol; 77.2% calculated for Ir).

Method B. A 100-mL Schlenk flask was charged with a 180-mg (0.268-mmol) sample of [Ir(COD)Cl]₂ and 30 mL of CH₃CN to form a yellow-orange slurry. CO was bubbled through the slurry for 5 min. During this time, the orange solid dissolved; the solution color changed to blue-green, and a blue-green precipitate formed. Under a N₂ atmosphere, a 100-mL Schlenk flask was charged with a 253-mg (1.610-mmol) sample of PTA and 30 mL of methanol to form a clear, colorless solution. Over a 1-min period, under an N₂ atmosphere, the PTA solution was added to the flask containing the blue-green precipitate. The reaction was allowed to stir under the CO/N₂ atmosphere for 30 min. During this time, the blue-green solid dissolved. The color changed to brown-orange and ultimately to greenish-yellow, and a pale green solid formed. To ensure complete precipitation, the excess CO was removed by bubbling N₂ through the solution for 10 min. The solid was collected on a medium frit, washed with MeOH (3 × 10 mL), and dried in vacuo (yield: 307 mg, 0.422 mmol; 78.7% calculated for Ir). Data for **1** are as follows. Anal. Calcd for IrClOP₃N₉C₁₉H₃₆·3C₂H₅OH (molecular weight, 865.36): C, 34.70; H, 6.29; N, 14.57. Found: C, 34.37; H, 5.91; N, 14.38. IR: ν (terminal CO) 1950 cm⁻¹. ³¹P{¹H} NMR (DMSO, 20 °C): δ -60.9 (int = 1, t, ²J_{P-P} = 12 Hz), -76.0 (int = 2, d, ²J_{P-P} = 12 Hz). FABMS (*m*-nitrobenzyl alcohol matrix): observed *m/z* 728.2 {calcd 728.2 for [Ir(PTA)₃(CO)Cl] plus H⁺ = M⁺}, 571.1 {calcd 571.0 for [M less (PTA)]⁺}, 543.1 {calcd 543.0 for [M less (PTA), (CO)]⁺}.

[Ir(PTA)₃(CO)Cl] (1**) and [Ir(PTA)₂(CO)Cl] (**2**).** This mixture was prepared by following the method B procedure described for **1** but with the use of 4 equiv of PTA (220 mg, 1.40 mmol)/equiv of [Ir(COD)Cl]₂ (235 mg, 0.350 mmol). Upon removal of the excess CO, yellow microcrystals of the mixture precipitated from the solution (yield: 454 mg, 0.350 mmol; 75.4% calculated for Ir). Data for the mixture of **1** and **2** are as follows. Anal. Repeated analyses of the crystalline solids were variable, indicative of the presence of a mixture of varying composition. IR: ν (terminal CO) 1935, 1950 cm⁻¹. ³¹P{¹H} NMR (DMSO, 20 °C): δ -58.1 ppm (s). FABMS (*m*-nitrobenzyl alcohol matrix): observed *m/z* 728.2 {calcd 728.2 for [Ir(PTA)₃(CO)Cl] plus H⁺ = M⁺}, 571.1 {calcd 571.0 for [M less (PTA)]⁺}, 543.1 {calcd 543.0 for [M less (PTA), (CO)]⁺}.

[Ir(PTA)₄(CO)]Cl (3**). Method A.** A 100-mL Schlenk flask was charged with a 53.5-mg (0.0686-mmol) sample of *trans*-[Ir(PPh₃)₂(CO)Cl], a 65.0-mg (0.415-mmol) sample of PTA and 50 mL of 95% ethanol to form a greenish yellow slurry. The slurry was heated to 60 °C to form a clear, pale green solution. The resulting system was allowed to stir for 4 h. Upon cooling to room temperature, the solvent volume was reduced to ≈10 mL. The resulting pale yellow-green

- (7) (a) Kalck, P.; Monteil, F. *Adv. Organomet. Chem.* **1992**, *34*, 219. (b) Borowski, A. F.; Cole-Hamilton, D. J.; Wilkinson, G. *New J. Chem.* **1978**, *2*, 137. (c) Southern, T. G. *Polyhedron* **1989**, *8*, 407. (d) Barton, M.; Atwood, J. D. *J. Coord. Chem.* **1991**, *24*, 43.
- (8) (a) Joo, F.; Kovacs, J.; Katho, A.; Benyei, A. C.; Decuir, T.; Darensbourg, D. J. *Inorg. Synth.* **1998**, *32*, 1. (b) Herrmann, W. A.; Kohlpainter, C. W. *Inorg. Synth.* **1998**, *32*, 8. (c) Roman, P. J., Jr.; Paterniti, D. P.; See, R. F.; Churchill, M. R.; Atwood, J. D. *Organometallics* **1997**, *16*, 1484. (d) Paterniti, D. P.; Roman, P. J., Jr.; Atwood, J. D. *Organometallics* **1997**, *16*, 3371.
- (9) Darensbourg, D. J.; Decuir, T. J.; Reibenspies, J. H. In *Aqueous Organometallic Chemistry and Catalysis*; Horvath, I. T., Joo, F., Eds.; NATO ASI Series 3/5; Kluwer: Dordrecht, 1995; p 61.
- (10) Darensbourg, D. J.; Robertson, J. B.; Larkins, D. L.; Reibenspies, J. H. *Inorg. Chem.* **1999**, *38*, 2473.
- (11) (a) Darensbourg, M. Y.; Daigle, D. *Inorg. Chem.* **1975**, *14*, 1217. (b) Alyea, E. C.; Fischer, K. J.; Foo, S.; Phillip, B. *Polyhedron* **1993**, *12*, 489. (c) Darensbourg, D. J.; Decuir, T. J.; Stafford, N. W.; Robertson, J. B.; Draper, J. D.; Reibenspies, J. H. *Inorg. Chem.* **1997**, *36*, 4218. (d) Muir, M. M.; Muir, J. A.; Alyea, E. C.; Fischer, K. J. *J. Crystallogr. Spectrosc. Res.* **1993**, *23*, 745. (e) Assefa, Z.; McBurnett, B. G.; Staples, R. J.; Fackler, J. P., Jr.; Assmann, B.; Angermaier, K.; Schmidbauer, H. *Inorg. Chem.* **1995**, *34*, 75. (f) Forward, J. M.; Assefa, Z.; Staples, R. J.; Fackler, J. P., Jr. *Inorg. Chem.* **1996**, *35*, 16. (g) Alyea, E. C.; Fischer, K. J.; Johnson, S. *Can. J. Chem.* **1989**, *67*, 1319. (h) Alyea, E. C.; Ferguson, G.; Kannan, S. *Polyhedron* **1998**, *17*, 2727.
- (12) (a) Darensbourg, D. J.; Joo, F.; Kannisto, M.; Katho, A.; Reibenspies, J. H. *Organometallics* **1992**, *11*, 1990. (b) Darensbourg, D. J.; Joo, F.; Kannisto, M.; Katho, A.; Reibenspies, J. H. *Inorg. Chem.* **1994**, *33*, 200. (c) Cermak, J.; Kuicalcova, M.; Blechta, V. *Collect. Czech. Chem. Commun.* **1997**, *62*, 355. (d) Pruchnik, F. P.; Smolenski, P.; Wajda-Hermanowicz, K. *J. Organomet. Chem.* **1998**, *570*, 63.
- (13) Pruchnik, F. P.; Smolenski, P.; Raksa, I. *Pol. J. Chem.* **1995**, *69*, 5.
- (14) Darensbourg, D. J.; Stafford, N. W.; Joo, F.; Reibenspies, J. H. *J. Organomet. Chem.* **1995**, *488*, 99.
- (15) Joo, F.; Nadasdi, L.; Benyei, A. C.; Darensbourg, D. J. *J. Organomet. Chem.* **1996**, *512*, 45.
- (16) Nadasdi, L.; Joo, F. *Inorg. Chim. Acta* **1999**, *293*, 218.

- (17) (a) Daigle, D. J. *Inorg. Synth.* **1998**, *32*, 40. (b) Daigle, D. J.; Pepperman, A. B.; Vail, S. L. *J. Heterocycl. Chem.* **1974**, *17*, 407.
- (18) Collman, J. P.; Sears, C. T., Jr.; Kubota, M. *Inorg. Synth.* **1990**, *28*, 90.
- (19) Herde, J. L.; Lambert, J. C.; Senoff, C. V. *Inorg. Synth.* **1974**, *15*, 18.

precipitate was collected on a medium frit under N₂, washed with benzene (3 × 10 mL), chloroform (3 × 10 mL), and diethyl ether (3 × 10 mL), and dried in vacuo (yield: 44.8 mg, 0.0507 mmol; 73.9% calculated for Ir).

Method B. A 100-mL Schlenk flask was charged with a 37.8-mg (0.0520-mmol) sample of **1**, a 29.8-mg (0.190 mmol) sample of PTA, and 40 mL of 95% ethanol to form a greenish yellow slurry. The slurry was heated to 60 °C and allowed to stir for 12 h. After cooling to room temperature, the solvent volume was reduced to 5 mL, and the resulting pale yellow-green precipitate was collected on a medium frit under N₂, washed with chloroform (3 × 10 mL) and diethyl ether (3 × 10 mL), and dried in vacuo (yield: 25.5 mg, 0.0288 mmol; 55.4% calculated for Ir). Data for **3** are as follows. Anal. Calcd for IrClO₄N₁₂C₂₅H₄₈·3H₂O (molecular weight, 938.35): C, 32.00; H, 5.80; N, 17.92. Found: C, 31.92; H, 5.82; N, 17.77. IR: ν (terminal CO) 1992 cm⁻¹. ¹H NMR (D₂O, 20 °C): δ 4.07 (int = 24, broad s) (PCH₂N); 4.52 (int = 24, m, ²J_{H–H} = 14 Hz) (NCH₂N). ³¹P{¹H} NMR (D₂O, 20 °C): δ -85.1 ppm (s). FABMS (*m*-nitrobenzyl alcohol matrix): observed *m/z* 849.1 {calcd 848.8 for [Ir(PTA)₄(CO)]⁺ = M⁺}, 821.2 {calcd 820.8 for [M less (CO)]⁺}, 692.1 {calcd 691.7 for [M less (PTA)]⁺}.

cis-[Ir(PTAH)₂(PTA)₂Cl₂]Cl₃ (4**) and cis-[Ir(PTAH)₄(H)₂]Cl₅ (**5**).** **Method A.** A 5-mL vial was charged with a 50.1mg (0.0579-mmol) sample of **1** and 1 mL of 0.1 M HCl. The resulting pale gray-green solution was placed in an acetone diffusion chamber, and a mixture of crystals developed over 3 days. Compound **4** may be separated from compound **5** by physical methods under the microscope. This is easily accomplished because **4** forms white, opaque, feather-like crystals (yield: 24.3 mg, 0.0235 mmol; 40.5% calculated for Ir) while **5** crystallizes as colorless needles (yield: 19.7 mg, 0.0193 mmol; 33.3% calculated for Ir). The data for **4** are as follows. Anal. Calcd for IrP₄Cl₅N₁₂C₂₄H₅₀·2H₂O (molecular weight 1036.19): C, 27.82; H, 5.25; N, 16.23. Found: C, 27.90; H, 5.22; N, 16.22. ¹H NMR (D₂O, 20 °C): δ 4.42 (int = 24, broad s) (PCH₂N), 4.56 (int = 24, broad s) (NCH₂N). ³¹P{¹H} NMR (D₂O, 20 °C): δ -72.6 (int = 1, t, ²J_{P–P} = 15 Hz), -87.8 (int = 1, t, ²J_{P–P} = 15 Hz). FABMS (*m*-nitrobenzyl alcohol matrix): observed *m/z* 891.3 {calcd 891.7 for [Ir(PTA)₂(PTA)₂Cl₂]⁺ = M⁺}, 857.3 {calcd 857.3 for [M less (Cl); plus (H)]⁺}, 823.3 {calcd 822.8 for [M less 2 (Cl); plus 2 (H)]⁺}, 734.2 {calcd 734.6 for [M less (PTA)]⁺}, 700.2 {calcd 700.2 for [M less (Cl), (PTA); plus (H)]⁺}. The data for **5** are as follows. Anal. Calcd for IrP₄Cl₅N₁₂C₂₄H₅₄·3H₂O–HCl (molecular weight, 1021.75): C, 28.21; H, 5.82; N, 16.45. Found: C, 28.31; H, 5.78; N, 16.50. IR: ν (Ir–H) 2016, 2036 cm⁻¹. ¹H NMR (D₂O, 20 °C): δ -13.79 (1 H, dq, ²J_{H–P_{trans}} = 120 Hz, ²J_{H–P_{cis}} = 22 Hz), -13.79 (1 H, dt, ²J_{H–P_{trans}} = 91 Hz, ²J_{H–P_{cis}} = 22 Hz), 4.19 (int = 16, d, ³J_{H–H} = 25 Hz) (NCH₂N⁺), 4.65 (int = 16, s) (PCH₂N), 4.72 (int = 8, s) (PCH₂N⁺), 4.74 (int = 8, s) (NCH₂N), 4.78 (int = 4, m) (H–N⁺). ³¹P{¹H} NMR (D₂O, 20 °C): δ -74.1 (int = 1, t, ²J_{P–P} = 18 Hz), -82.4 (int = 1, t, ²J_{P–P} = 18 Hz). FABMS (*m*-nitrobenzyl alcohol matrix): observed *m/z* 823.3 {calcd 823.9 for [Ir(PTA)₃(PTAH)(H)₂]²⁺ = M⁺}, 662.6 {calcd 663.1 for [M less (PTAH), 2(H)]}.

cis-[Ir(PTAH)₂(PTA)₂Cl₂]Cl₃ (4**) and cis-[Ir(PTAH)₄(H)₂]Cl₅ (**5**).** **Method B.** A mixture of white, opaque, feather-like crystals, **4** (yield: 23.6 mg, 0.0228 mmol; 42.0% calculated for Ir) and colorless needles, **5** (yield: 26.5 mg, 0.0259 mmol; 47.7% calculated for Ir) was prepared by following the same procedure as that described in Method A except that a 48.0-mg (0.0543-mmol) sample of **3** was used in place of **1**.

cis-[Ir(PTAD)₂(PTA)₂Cl₂]Cl₃ (4b**) and cis-[Ir(PTAD)₄(D)₂]Cl₅ (**5b**).** **Method C.** A 5-mL vial was charged with a 51.1-mg (0.0578-mmol) sample of **3** and 1 mL of 0.1 M DCl in D₂O in the presence of O₂. The resulting yellow solution was placed in an acetone diffusion chamber. A mixture of white, opaque, feather-like crystals of **4b** (yield: 21.2 mg, 0.0203 mmol; 35.2% calculated for Ir) and colorless needles of **5b** developed over 3 days (yield: 26.6 mg, 0.0263 mmol; 45.5% calculated for Ir). The data for **4** are as follows. Anal. Calcd for IrP₄Cl₅N₁₂C₂₄H₄₈D₂·2D₂O (molecular weight, 1042.22): C, 27.66; H, 5.80; N, 16.13. Found: C, 27.60; H, 5.75; N, 16.09. The data for **5b** are as follows. Anal. Calcd for IrP₄Cl₅N₁₂C₂₄H₄₈D₄·D₂O–2DCl (molecular weight, 955.29): C, 30.17; H, 6.33; N, 17.60. Found: C, 30.09; H, 6.27; N, 17.56. IR: ν (Ir–D) 1457 cm⁻¹.

Table 1. Crystallographic Data for [Ir(PTA)₄(CO)]Cl·3H₂O (**3**) and [Ir(PTAH)₃(PTAH₂(H)₂)Cl₆·6H₂O·H₃OCl (**5**)

	3 Cl	5 (6 Cl)
Crystal Parameters and Measurement of Intensity Data		
formula	IrClP ₄ O ₄ N ₁₂ C ₂₅ H ₅₄	IrCl ₇ P ₄ O ₇ N ₁₂ C ₂₄ H ₇₂
fw amu	938.33	1205.17
space group	<i>Pbca</i>	<i>P1</i>
cell params at <i>T</i> , K	173	173
<i>a</i> , Å	20.3619(4)	12.4432(9)
<i>b</i> , Å	14.0345(3)	12.5921(9)
<i>c</i> , Å	24.1575(5)	16.3231(12)
α , deg	90	76.004(1)
β , deg	90	71.605(1)
γ , deg	90	69.177(1)
<i>V</i> , Å ³	6903.5(2)	2244.0(3)
<i>Z</i>	8	2
calcd density, Mg m ⁻³	1.806	1.784
abs coeff, mm ⁻¹	4.184	3.589
radiation wavelength, Å	0.71073	0.71073
Refinement ^a by Full-Matrix Least Squares ^b on <i>F</i> ²		
R1	0.0246	0.0423
wR2	0.0574	0.1117

^a Relevant equations are: R1 = $\sum|F_o| - |F_c|/\sum|F_o|$, wR2 = $\{\sum[w(F_o^2 - F_c^2)^2]/\sum[w(F_o^2)^2]\}^{1/2}$, where $w = 1/\sigma^2(F_o^2) + (a^*p)^2 + b^*p$.

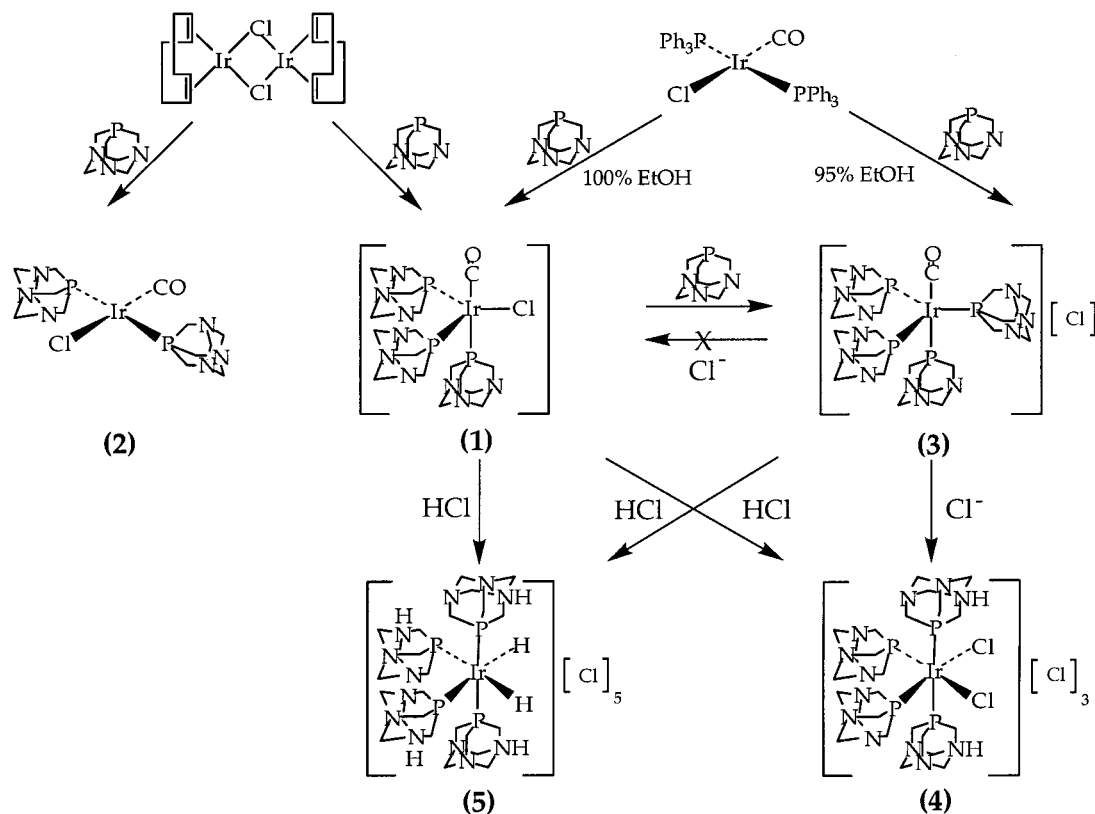
^b Refinements are performed with *F*² (rather than *F*), enabling all data to be used, with the result that the experimental information is more fully exploited.

cis-[Ir(PTAH)₂(PTA)₂Cl₂]Cl₃ (4**).** **Method D.** A 10-mL vial was charged with a 49.5-mg (0.0560-mmol) sample of **3**, a 16.4-mg (0.281-mmol) sample of NaCl, and 5 mL of MeOH and the mixture was allowed to stir overnight in the presence of O₂. The resulting white precipitate was collected on a medium frit under N₂, washed with methanol (3 × 10 mL) and diethyl ether (3 × 10 mL), and dried in vacuo (yield: 21.8 mg, 0.0235 mmol; 42.0% calculated for Ir).

Reaction of [Ir(PTA)₄(CO)]Cl (3**) with Anhydrous HCl.** A 100-mL Schlenk flask was charged with a 47.4-mg (0.0536-mmol) sample of [Ir(PTA)₄(CO)]Cl (**3**) and 15 mL of absolute ethanol to form a pale green slurry. Upon the addition of 0.54 mL of 1.0 M HCl (0.54 mmol) in Et₂O, the slurry turned white. After the mixture was stirred for 1 h, the precipitate was collected on a medium frit under N₂, washed with diethyl ether (3 × 10 mL), and dried in vacuo (yield: 46.2 mg). The IR, ¹H NMR, and ³¹P NMR data indicated the presence of complexes **4**, **5**, and [Ir(PTA)₄(H)(Cl)]⁺ (**6**). The data for **6** are as follows. ν (Ir–H) 2075 cm⁻¹. ¹H NMR (D₂O, 20 °C): δ -12.00 (dq, ²J_{H–P_{trans}} = 139 Hz, ²J_{H–P_{cis}} = 19 Hz). ³¹P{¹H} NMR (D₂O, 20 °C): δ -65.7 (int = 1, dt, ²J_{P–P} = 19 Hz, ²J_{P–P} = 17 Hz), -83.5 (int = 2, t, ²J_{P–P} = 19 Hz), -91.7 (int = 1, broad t, ²J_{P–P} = 19 Hz).

X-ray Structure Determinations of [Ir(PTA)₄(CO)]Cl (3**) and [Ir(PTAH)₃(PTAH₂(H)₂)Cl₆ (**5**).** Collection and Reduction of Data. Summaries of crystallographic data for **3** and **5** are presented in Table 1 and as Supporting Information. Samples of **3** and **5** desolvated over time upon exposure to air. Therefore, the crystals of **3** and **5**, which were selected for analysis, were attached to a small glass fiber and immediately mounted on the Siemens SMART CCD area detector system for data collection at 173 K. An initial set of cell constants was calculated for **3** from reflections harvested from three sets of 20 frames. These initial sets of frames were oriented such that orthogonal wedges of reciprocal space were surveyed. This produced orientation matrixes determined from 207 reflections. Final cell constants were calculated from a set of 8192 strong reflections from the actual data collection. In this hemispheric collection, a randomly oriented region of reciprocal space was surveyed to the extent of 1.3 hemispheres to a resolution of 0.84 Å. Three major swaths of frames were collected with 0.30° steps in ω for the sample. For compound **5**, intensity data were collected using the ω scan technique to a maximum of 2 θ value of 55° using 10-s exposures. Final cell constants were again calculated from a set of 8192 strong reflections. A numerical absorption correction was applied based on the crystal shape.

Solution and Refinement of Structures. The structures of **3** and **5** were determined by successful direct-methods solutions, which provided

Scheme 1. Synthesis of PTA Ligated Ir Complexes

most non-hydrogen atoms from the respective E-maps. Several full-matrix least-squares/difference Fourier cycles were performed that located the remainder of the non-hydrogen atoms for **3**. For **5**, the remainder of the non-hydrogen atoms were located after several cycles of structure expansion and full-matrix least-squares refinement. In both structures, all non-hydrogen atoms were refined with anisotropic displacement parameters. All hydrogen atoms of **3** were placed in ideal positions and refined as riding atoms with relative isotropic displacement parameters while the protons of the water solvates were refined positionally with relative isotropic displacement parameters. The carbon-bound hydrogen atoms of **5** were refined as riding atoms with group isotropic displacement parameters fixed at $1.2 \times U(\text{eq})$ of the host carbon atom. Hydrogen atoms bound to nitrogen were identified from difference Fourier maps and were refined with a riding model. The hydride ligands were also identified from difference Fourier maps and were allowed to freely refine with a common isotropic displacement parameter. Hydrogen atoms bound to several oxygens, including O1, O2 (a formal hydronium ion), O4, and O5, were identified from difference Fourier maps, and were refined using a riding model. Hydrogen atoms bound to the other oxygens (O3, O6, and O7) were not identified, and no effort was made to place them at calculated positions. However, these six hydrogen atoms are included in calculations of the empirical formula, crystal density, $F(000)$, and the absorption coefficient. The water molecule centered on O7 was located near an inversion center and was found to be statistically disordered over two positions.

Compound **3** crystallized in the space group $Pbca$ according to systematic absences and intensity statistics. The structure was found as expected as a cation with one chloride anion and three waters per asymmetric unit. There is one large difference Fourier peak near the Ir(1) position. Several different absorption corrections were tried, but none improved the situation. It appears that this feature may be an artifact of $\lambda/2$ contamination. This problem has been observed in a few previous structures where third-row transition or actinide metals were present.

Compound **5** crystallized in the space group $P\bar{1}$. During refinement of the structure, it became apparent that there were a total of seven fully occupied chloride ions in the asymmetric unit. This negative charge

is balanced by a hexacationic iridium(III) complex and a single hydrated proton cluster, formally $[\text{H}_3\text{O}^+ \cdot 2\text{H}_2\text{O}]$, which is hydrogen bonded to one of the seven chloride ions ($\text{Cl}2$). There are extensive hydrogen-bonding interactions in the unit cell involving the seven chloride ions, six water molecules, the hydronium ion, and the iridium(III) complex. Representations of this are provided in the Supporting Information. The final difference map featured one large peak ($3.31 \text{ e}^-/\text{\AA}^3$) located 1.06 \AA from the iridium center. This may arise from $\lambda/2$ contamination or an incomplete absorption correction.

Results and Discussion

Synthesis and Characterization of $[\text{Ir}(\text{PTA})_3(\text{CO})\text{Cl}]$ (1). The reactions observed in this study are summarized in Scheme 1 and described in the Experimental Section. Characterization data for compounds **1–5** are included in the Experimental Section and, when appropriate, discussed below. The 1,3,5-triaza-7-phosphaadamantane ligated complex, $[\text{Ir}(\text{PTA})_3(\text{CO})\text{Cl}]$ (**1**), was produced in 54% yield by reacting $\text{trans-}[\text{Ir}(\text{PPh}_3)_2(\text{CO})\text{Cl}]^{18}$ with 3 equiv of PTA¹⁷ for 12 h at 78°C as an absolute ethanol slurry. During this time, the color of the slurry changed from greenish yellow to produce **1** as an air-stable, pale yellow solid (Scheme 1). The yield of this reaction may be increased to 77% by performing the same experiment with 6 equiv of PTA. As indicated by ^{31}P NMR, the lower yield with 3 equiv is due to the formation of mixed phosphine complexes. The problem of producing PPh_3/PTA complexes may be alleviated by synthesizing **1** from a different Ir source. The reaction of $[\text{Ir}(\text{COD})\text{Cl}]_2$ under an atmosphere of CO with 6 equiv of 1,3,5-triaza-7-phosphaadamantane produces $[\text{Ir}(\text{PTA})_3(\text{CO})\text{Cl}]$ (**1**) as an air-stable, pale green powder in 78% yield (Scheme 1).

The empirical formula of **1** was confirmed by fast atom bombardment-mass spectrometry and elemental analysis data. $[\text{Ir}(\text{PTA})_3(\text{CO})\text{Cl}]$ (**1**) is only sparingly soluble in DMSO, insoluble in acetonitrile, acetone, alcohols, and ethers, and

reactive with water and dilute HCl, *vide infra*. Therefore, it was not possible to grow crystals of **1** and elucidate its structure via X-ray analysis. Its geometry, however, may be determined from its spectroscopic data. In the IR spectrum, the CO stretching frequency ($\nu_{\text{CO}} = 1950 \text{ cm}^{-1}$) is substantially higher than that of other $[\text{IrP}_3(\text{CO})\text{Cl}]$ systems in which the CO is equatorially coordinated.²⁰ This indicates that the CO moiety is axially ligated. Axial coordination would limit the degree of back-donation into the π^* orbital of CO, and consequently, the CO stretch would be higher. Axial CO ligation has recently been crystallographically observed in the related compounds, $[\text{Ir}(\text{PTAME})_3(\text{CO})\text{I}](1)_3$ (PTAME = 1-methyl-3,5-diaza-1-azonia-7-phosphatricyclo[3.3.1.1]decane)²¹ and $[\text{Ir}(\text{PTA})_4(\text{CO})\text{Cl}]$ (**3**), *vide infra*. The room temperature $^{31}\text{P}\{^1\text{H}\}$ NMR spectrum of **1** in DMSO contains a triplet ($\delta = -60.9 \text{ ppm}$, $^2J_{\text{P-P}} = 12 \text{ Hz}$) and a doublet ($\delta = -76.0 \text{ ppm}$, $^2J_{\text{P-P}} = 12 \text{ Hz}$) in a respective 1 to 2 ratio. Therefore, two phosphines must occupy equatorial sites while the third resides in the other axial position. Consequently, the third equatorial site must be filled by the chloride ligand. This overall configuration seems logical because electronegative atoms prefer to occupy equatorial positions in d^8 systems.²² Furthermore, the small cone angle (103°)¹⁰ of 1,3,5-triaza-7-phosphaadamantane would facilitate a 90° orientation of the PTA ligands.

Synthesis and Characterization of a Mixture of $[\text{Ir}(\text{PTA})_3(\text{CO})\text{Cl}]$ (1**) and $[\text{Ir}(\text{PTA})_2(\text{CO})\text{Cl}]$ (**2**).** It is important to discuss the $[\text{Ir}(\text{COD})\text{Cl}]_2$ reaction when only 2 equiv of PTA are used per Ir. This is essentially the general procedure described by Burk and Crabtree for the preparation of phosphine derivatives of Vaska's compound.²³ This reaction produces a bright yellow, microcrystalline solid whose IR spectrum contains two CO stretching frequencies in approximately a 50:50 ratio. The band at 1950 cm^{-1} corresponds to **1**, while the band at 1939 cm^{-1} is due to something different and is very similar to that of *trans*- $[\text{Ir}(\text{PMe}_3)_2(\text{CO})\text{Cl}]$ ($\nu_{\text{CO}} = 1940 \text{ cm}^{-1}$).²⁴ Therefore, upon consideration of the stoichiometry of the reaction and this stretching frequency, it is assumed that the reaction of $[\text{Ir}(\text{COD})\text{Cl}]_2$ with 4 equiv of PTA under an atmosphere of CO produces a mixture of **1** and **2**. This theory is substantiated by fast atom bombardment-mass spectrometry. The mass spectrum of the mixture is identical to that of **1**, which indicates that a dicarbonyl is not present. Additionally, complex **1** is known to fragment into $[\text{Ir}(\text{PTA})_2(\text{CO})\text{Cl}]$ in the mass spectrometer (see experimental results), and this action would mask the presence of **2**. Repeated elemental analyses of the mixture were varied and, therefore, inconclusive. Variation in the elemental analysis is not surprising upon consideration of the consequences of a slight change in the relative percentages of **1** and **2**. The presence of a mixture seems incongruent with the ^{31}P NMR data, which contains only 1 resonance, a singlet at -58.1 ppm . Only one species is observed in solution because $[\text{Ir}(\text{PTA})_3(\text{CO})\text{Cl}]$ (**1**) is only slightly soluble in DMSO while, as evidenced by the yellow color, $[\text{Ir}(\text{PTA})_2(\text{CO})\text{Cl}]$ (**2**) is moderately soluble. Therefore, when the sample is filtered into an NMR tube, most of the $[\text{Ir}(\text{PTA})_3(\text{CO})\text{Cl}]$ is separated as insoluble solid, and the trace amount that has dissolved is lost as spectral background. Work is presently being done to isolate compound **2** as a pure

solid; however, all initial attempts have produced a nearly 50/50 mixture of **1** and **2**, according to IR. This is presumably due to an equilibrium between **1** and **2**:



Synthesis and Characterization of $[\text{Ir}(\text{PTA})_4(\text{CO})\text{Cl}]$ (3**).** In aqueous solution, $[\text{Ir}(\text{PTA})_3(\text{CO})\text{Cl}]$ (**1**) rapidly converts into the tetraphosphino complex, $[\text{Ir}(\text{PTA})_4(\text{CO})\text{Cl}]$ (**3**). The formation of **3** may be explained by invoking an equilibrium between **1** and the reactive, 16-electron species $[\text{Ir}(\text{PTA})_3(\text{CO})]^+$:



Halpern suggested a similar scenario with a comparable complex, $[\text{Ir}(\text{PMe}_2\text{Ph})_3(\text{CO})\text{Cl}]$.²⁵ Such an equilibrium is reasonable in water because the hydration of Cl^- would enthalpically favor chloride dissociation.²⁶ The resulting, square planar complex, $[\text{Ir}(\text{PTA})_3(\text{CO})]^+$, could easily add a fourth PTA ligand to form $[\text{Ir}(\text{PTA})_4(\text{CO})\text{Cl}]$ (**3**). This extra phosphine is presumably from the equilibrium between **1** and **2** (*vide supra*).

$[\text{Ir}(\text{PTA})_4(\text{CO})\text{Cl}]$ (**3**) may also be formed by the reaction of **1** with 1 equiv of PTA in 95% EtOH (Scheme 1) or by refluxing Vaska's compound, *trans*- $[\text{Ir}(\text{PPh}_3)_2(\text{CO})\text{Cl}]$, with 6 equiv of PTA in 95% ethanol (Scheme 1). Interestingly, the latter of these processes is almost identical to that which produces complex **1**. In the synthesis of **3**, however, a small amount of water is present that allows all species to dissolve. Presumably, this causes $[\text{Ir}(\text{PTA})_3(\text{CO})\text{Cl}]$ (**1**) to be formed in situ, and subsequent chloride dissociation allows a fourth phosphine to add as discussed above.

Complex **3** has an appreciable solubility in H_2O ($6 \times 10^{-2} \text{ M}$) while also being sparingly soluble in DMSO and methanol but insoluble in other alcohols, halogenated hydrocarbons, diethyl ether, acetonitrile, and benzene. The empirical formula was determined via elemental analysis and fast atom bombardment-mass spectrometry. The presence of a terminal CO is supported by the IR spectrum, which shows a $\text{C}\equiv\text{O}$ stretching frequency at 1992 cm^{-1} . In the room temperature $^{31}\text{P}\{^1\text{H}\}$ NMR spectrum, a single, sharp resonance is observed at -89.4 ppm . This indicates that **3** must undergo rapid rearrangement at room temperature via Barry-pseudo rotation. Unfortunately, lack of solubility in an appropriate solvent precluded low-temperature NMR work from being done to elucidate its structure in solution. Its solid-state structure, however, was determined via single-crystal X-ray diffraction.

Solid-State Structure of $[\text{Ir}(\text{PTA})_4(\text{CO})\text{Cl}]$ (3**).** X-ray quality crystals of **3** were grown by slow diffusion of EtOH into an aqueous solution of $[\text{Ir}(\text{PTA})_4(\text{CO})\text{Cl}]$. Complex **3** was found to crystallize in the *Pbca* space group, and the structure of the cation is shown in Figure 1. Selected interatomic distances and angles are given in Table 2. Additional crystallographic data are provided as Supporting Information. The coordination geometry about the iridium atom is trigonal bipyramidal with the three equatorial sites filled by the phosphorus atoms of three PTA ligands and the axial sites occupied by the phosphorus atom of another phosphine and the carbon atom of CO. This structure is very similar to a related Rh–PTA complex, $[\text{Rh}(\text{PTAH})_3(\text{PTA})\text{Cl}]\text{Cl}_3$, in which the chloride occupies an axial

(20) (a) Sigel, W. O.; Lapporte, S. J.; Collman, J. P. *Inorg. Chem.* **1971**, *10*, 2158. (b) Chen, J. Y.; Halpern, J.; Molin-Case, J. *J. Coord. Chem.* **1973**, *2*, 239. (c) Janser, P.; Venanzi, L. M.; Bachechi, F. *J. Organomet. Chem.* **1985**, *296*, 229. (d) Mayer, H. A.; Stobel, P.; Fawzi, R.; Steimann, M. *Chem. Ber.* **1995**, *128*, 719.

(21) Krogstad, D. A.; Halfen, J. A. Unpublished results.

(22) Rossi, A. R.; Hoffmann, R. *Inorg. Chem.* **1975**, *14*, 365.

(23) Burk, M. J.; Crabtree, R. H. *Inorg. Chem.* **1986**, *25*, 931.

(24) Labinger, J. A.; Osborn, J. *Inorg. Synth.* **1978**, *18*, 62.

(25) Chen, J. Y.; Halpern, J. *J. Am. Chem. Soc.* **1971**, *93*, 4939.

(26) (a) The enthalpy of hydration of Cl^- is -77 kcal/mol . Sienko, M. J.; Plane, R. A. *Chemical Principles and Properties*, 2nd ed.; McGraw-Hill, Inc.: New York, 1974; Chapter 8. (b) Burke, N. E.; Singhal, A.; Hintz, M. J.; Ley, J. A.; Hui, H.; Smith, L. R.; Blake, D. M. *J. Am. Chem. Soc.* **1979**, *101*, 74.

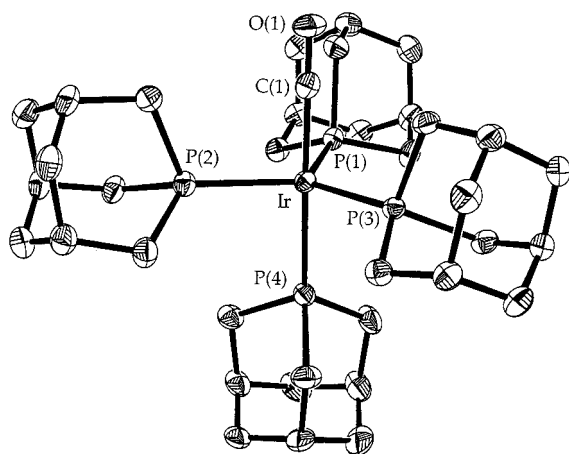


Figure 1. Thermal ellipsoid representation of $[\text{Ir}(\text{PTA})_4(\text{CO})]\text{Cl}\cdot 3\text{H}_2\text{O}$ (**3**) showing the atom-labeling scheme. Thermal ellipsoids are drawn at the 50% probability level.

Table 2. Selected Bond Distances (Å) and Bond Angles (deg) with Estimated Standard Deviations for $[\text{Ir}(\text{PTA})_4(\text{CO})]\text{Cl}\cdot 3\text{H}_2\text{O}$ (**3**)

Bond Distances			
Ir—C1	1.895 (4)	Ir—P2	2.3188 (9)
C1—O1	1.138 (4)	Ir—P3	2.3187 (10)
Ir—P1	2.3229 (10)	Ir—P4	2.3378 (9)
Bond Angles			
Ir—C1—O1	179.8 (3)	P4—Ir—P1	92.02 (4)
C1—Ir—P1	87.22 (11)	P4—Ir—P2	93.87 (3)
C1—Ir—P2	87.31 (11)	P4—Ir—P3	93.09 (4)
C1—Ir—P3	86.52 (11)	P1—Ir—P2	118.79 (4)
C1—Ir—P4	178.80 (11)	P1—Ir—P3	121.51 (3)
		P3—Ir—P3	118.89 (3)

site.¹⁴ The angles between the equatorial phosphines (118.79(4)°, 118.89(3)°, and 121.51(3)°) of $[\text{Ir}(\text{PTA})_4(\text{CO})]\text{Cl}$ are very close to 120° while the angle between the axial ligands (178.80°) is also very close to that of the ideal geometry. As is shown in Figure 1, the Ir—P₃ moiety is not quite planar. This is due to steric crowding of the axial phosphine (P4) as indicated by the P(4)—Ir—P(X) angles, which are all greater than 90°.

This is the first reported $[\text{IrP}_4(\text{CO})]^+$ structure in which the CO is axially coordinated. Because of its excellent π -accepting ability, the CO has, up until this time, only been observed in the equatorial position.²⁷ This “new” orientation may be a consequence of the characteristics of PTA and the preferences of five-coordinate d⁸ complexes. According to calculations by Rossi and Hoffmann, the presence of electrons in the equatorial orbitals of d⁸ systems causes more electronegative moieties to favor the equatorial positions.²² Because of its π -accepting ability,^{11b} small size,¹⁰ and the presence of three electronegative nitrogen atoms, PTA is able to get close to the Ir center, accept electron density from the metal, and delocalize the charge. Presumably, this interaction is stronger than the π -bonding between CO and Ir; therefore, CO is relegated to occupying the axial site.

The axial ligation of CO in $[\text{Ir}(\text{PTA})_4(\text{CO})]\text{Cl}$ (**3**) causes its Ir—C bond to be weaker than that of other $[\text{IrP}_4(\text{CO})]^+$ systems.²⁷ This weakening may be observed by comparing the CO stretching frequency of **3** with the corresponding datum of $[\text{Ir}(\text{dppe})_2(\text{CO})]^+$ (dppe = 1,2-diphenylphosphinoethane).^{27a} The

CO in $[\text{Ir}(\text{dppe})_2(\text{CO})]^+$ is equatorially coordinated, and its CO stretching frequency (1933 cm⁻¹) is 59 cm⁻¹ lower than that of **3** (1992 cm⁻¹). These data indicate that the π^* orbital of CO in $[\text{Ir}(\text{PTA})_4(\text{CO})]^+$ (**3**) experiences less π -back-donation as a consequence of minimal Ir—CO overlap in the axial site. This poor orbital overlap allows the CO of **3** to be quite labile (vide infra).

Synthesis and Characterization of a Mixture of *cis*- $[\text{Ir}(\text{PTAH})_2(\text{PTA})_2\text{Cl}_2]\text{Cl}_3$ (4**) and *cis*- $[\text{Ir}(\text{PTAH})_4(\text{H})_2]\text{Cl}_5$ (**5**).** Previous researchers have shown that PTA complexes may be recrystallized upon protonation of the ligand.^{10,11c,12a,b,14} Therefore, in an effort to prepare $[\text{Ir}(\text{PTA})_3(\text{CO})\text{Cl}]$ (**1**) in a form suitable for X-ray crystallography, a solid sample of the compound was dissolved in 0.1 M HCl and acetone allowed to diffuse into the resultant solution. This procedure did not result in the isolation of a crystalline, protonated form of a **1**, but instead in the production of two new compounds, **4** and **5**. These new complexes were readily separated by inspection due to their different crystal habits. Investigation of these compounds by FAB-MS and elemental analysis provided their empirical formulas, $[\text{Ir}(\text{PTAH})_2(\text{PTA})_2\text{Cl}_2]\text{Cl}_3$ (**4**) (PTAH = protonated PTA) and $[\text{Ir}(\text{PTAH})_3(\text{PTA})(\text{H})_2]\text{Cl}_4$ (**5**). In this reaction, the phosphine is the limiting reagent. ³¹P NMR analysis of the mother liquor shows traces of **4** and **5** and the oxidized phosphine, PTAO (1,3,5-triaza-7-phosphatricyclodecane-7-oxide). Therefore, it is believed that the leftover Ir is ligated by Cl⁻ and/or H₂O.

Spectroscopic characterization of **4** provided significant insights into its structure. The FTIR spectrum of **4** lacks a band attributable to ν_{CO} , a feature that dominates the FTIR spectrum of its precursor **1**. The geometry of **4** was deduced by analysis of its ³¹P{¹H} NMR spectrum, which contains two triplets of equal intensity (δ = -72.6 (²J_{P-P} = 15 Hz), -87.8 (²J_{P-P} = 15 Hz) ppm. Such a spectrum is indicative of an octahedral geometry at Ir, in which two chloride ligands occupy *cis* coordination positions and PTA ligands (or its protonated congener) occupy the remaining sites. A similar structure was observed in the analogous Ru complex, $[\text{Ru}(\text{PTAH})_2(\text{PTA})_2\text{Cl}_2]\text{Cl}_2$,^{12b} in which two *cis* chloride ligands and two PTAs form the equatorial plane and the two axial sites are occupied by protonated phosphines.

The IR and NMR spectral data of **5** are also vital to its structural determination. As with complex **4**, the IR spectrum does not contain a CO stretch. It does, however, possess two bands of equal intensity at 2016 and 2036 cm⁻¹, which are consistent with the presence of an Ir—H moiety. This doublet may be explained by the symmetric and antisymmetric combinations of two Ir—H vibrations within the same molecule or by the presence of a mixture of two closely related monohydride complexes. Further insight into the nature of the Ir—H moiety in this complex was obtained via deuterium labeling experiments. We observed that the hydride ligands of $[\text{Ir}(\text{PTAH})_4(\text{H})_2]\text{Cl}_5$ (**5**) were inert toward Ir—H(D) exchange upon treatment with 0.10 M DCl in D₂O for 3 days. However, deuterium incorporation was observed when $[\text{Ir}(\text{PTA})_4(\text{CO})]\text{Cl}$ (**3**) was treated with DCl in D₂O ($\nu_{\text{Ir-D}}$ = 1457 cm⁻¹: symmetric and antisymmetric combinations not resolved; Ir—H/Ir—D calc'd = 1.405, observed = 1.391).

The possibility of the presence of two closely related monohydride complexes is discounted by analysis of the combined ³¹P and ¹H NMR data. The ³¹P{¹H} NMR spectrum of **5** (25 °C, D₂O) contains two triplets of equal intensity (δ = -74.1 ppm, ²J_{P-P} = 18 Hz; δ = -82.4 ppm, ²J_{P-P} = 18 Hz), which is consistent with an octahedral geometry in which two

(27) (a) Vaska, L.; Catone, D. L. *J. Am. Chem. Soc.* **1966**, *88*, 5324. (b) Jarvis, J. A. J.; Mais, R. H. B.; Owston, P. G.; Taylor, K. A. *J. Chem. Soc., Chem. Commun.* **1966**, 906. (c) Balch, A. L.; Catalano, V. J.; Olmstead, M. M. *J. Am. Chem. Soc.* **1990**, *112*, 2010. (d) Balch, A. L.; Catalano, V. J.; Noll, B. C.; Olmstead, M. M. *J. Am. Chem. Soc.* **1990**, *112*, 7558.

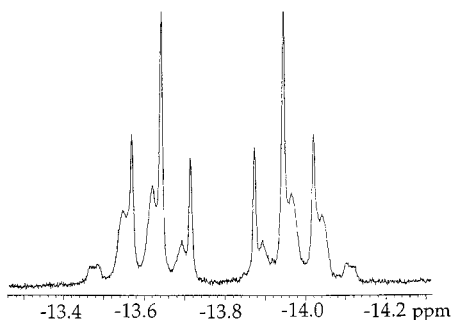


Figure 2. Partial ^1H NMR spectrum (hydride region) of $[\text{Ir}(\text{PTAH})_4(\text{H})_2]\text{Cl}_4$ (**5**) (300 MHz, 298 K) in D_2O .

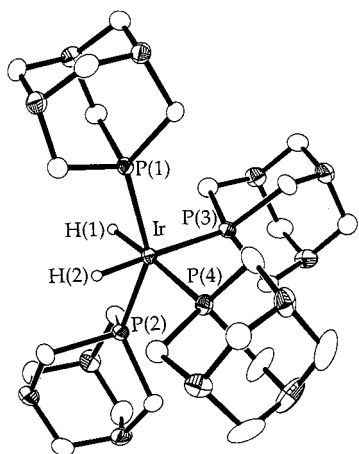


Figure 3. Thermal ellipsoid representation of the cationic structure of $[\text{Ir}(\text{PTAH})_3(\text{PTAH}_2)(\text{H})_2]\text{Cl}_6 \cdot 6\text{H}_2\text{O} \cdot \text{H}_3\text{OCl}$ (**5**) with C-bound H omitted for clarity. Thermal ellipsoids are drawn at the 50% probability level.

hydride ligands are in a *cis* configuration. Interpretation of the ^1H NMR spectrum (25 °C, D_2O) is more complex. As shown in Figure 2, the upfield region of this spectrum contains two overlapping multiplets of equal intensity, the combined integration of which indicates the presence of two hydride ligands per complex. The presence of these two multiplets (δ -13.79, dq, $^2J_{\text{H-P}_{\text{trans}}} = 120$ Hz, $^2J_{\text{H-P}_{\text{cis}}} = 22$ Hz; δ -13.79, dt, $^2J_{\text{H-P}_{\text{trans}}} = 91$ Hz, $^2J_{\text{H-P}_{\text{cis}}} = 22$ Hz) may be rationalized by invoking a slow equilibration between two closely related geometries. The doublet of quartets, which exhibits a strong $^2J_{\text{H-P}_{\text{trans}}}$ (120 Hz), is consistent with an idealized *cis*-dihydride octahedral geometry. The presence of the doublet of triplets, with its associated $^2J_{\text{H-P}_{\text{trans}}}$ (91 Hz), may be explained by invoking a distorted octahedral, C_{2v} like structure²⁸ in which the axial phosphines are bent toward the hydrides (Figure 3). A similar C_{2v} like, distorted octahedral geometry was observed in the structurally characterized complex, $[\text{Ir}(\text{PMe}_3)_4(\text{H})_2]^+$.²⁹ The proton NMR spectrum of $[\text{Ir}(\text{PMe}_3)_4(\text{H})_2]^+$ also contains a doublet of triplets in the hydride region. Therefore, the combined analytical and spectroscopic data indicate that **5** is a *cis*-dihydrido complex with a distorted octahedral geometry.

Solid-State Structure of $[\text{Ir}(\text{PTAH})_3(\text{PTAH}_2)(\text{H})_2]\text{Cl}_6 \cdot 6\text{H}_2\text{O} \cdot \text{H}_3\text{OCl}$ (5**).** Using the needles harvested from the reaction vial, complex **5** was found to crystallize in the $P\bar{1}$ space group. The structure of the cation is shown in Figure 3. Selected interatomic distances and angles are given in Table 3. Additional

Table 3. Selected Bond Distances (Å) and Bond Angles (deg) with Estimated Standard Deviations for $[\text{Ir}(\text{PTAH})_3(\text{PTAH}_2)(\text{H})_2]\text{Cl}_6 \cdot 6\text{H}_2\text{O} \cdot \text{H}_3\text{OCl}$ (**5**)

Bond Distances			
Ir–H1	1.43 (6)	Ir–P2	2.2847 (13)
Ir–H2	1.44 (6)	Ir–P3	2.3410 (14)
Ir–P1	2.2929 (13)	Ir–P4	2.3353 (14)
Bond Angles			
H1–Ir–P1	78 (3)	H1–Ir–H2	89 (4)
H1–Ir–P2	78 (2)	P1–Ir–P2	148.54 (5)
H1–Ir–P3	89 (3)	P1–Ir–P3	101.64 (5)
H1–Ir–P4	174 (3)	P1–Ir–P4	100.46 (5)
H2–Ir–P1	81 (2)	P2–Ir–P3	98.06 (5)
H2–Ir–P2	79 (3)	P2–Ir–P4	101.39 (5)
H2–Ir–P3	176 (3)	P3–Ir–P4	96.54 (5)
H2–Ir–P4	85 (3)		

crystallographic data are provided as Supporting Information. The overall stoichiometry identified in the crystalline sample of **5** was $[\text{Ir}(\text{PTAH})_3(\text{PTAH}_2)(\text{H})_2]\text{Cl}_6 \cdot 6\text{H}_2\text{O} \cdot \text{H}_3\text{OCl}$. The presence of seven chloride ions in the asymmetric unit coupled with a central Ir(III) ion and its two hydrido ligands dictates that six additional positive charges are required to achieve charge neutrality. Five of these positive charges are assigned to protonated PTA ligands, three monoprotated, and one doubly protonated. The remaining positive charge resides in a hydrated proton cluster. This assignment is based on the observation of a pyramidal H_3O^+ ion (centered on O2) in difference Fourier maps and the strong hydrogen-bonding interactions observed among this pyramidal ion, two adjacent water molecules (O1, O3; $\text{O2} \cdots \text{O}(\text{water}) = 2.7\text{--}2.8$ Å), and a chloride ion ($\text{Cl2}; \text{O2} \cdots \text{Cl2} = 3.08$ Å). Similar hydrated proton clusters have been previously observed in the solid-state structures of several acid hydrates.³⁰ Definitive assignment of the structure of this cluster awaits analysis by neutron diffraction.

The coordination geometry about the iridium atom is a distorted octahedron with two hydride ligands in a *cis* configuration, a geometry which resembles that of other $[\text{IrP}_4\text{H}_2]^{3+}$ complexes.^{29,31} It is believed that the steric repulsion between the phosphines forces the structure away from ideality. This is substantiated by the facts that all $\text{P}(1)\text{--Ir--P}(X)$ ($X = 3, 4$) and $\text{P}(2)\text{--Ir--P}(X)$ ($X = 3, 4$) angles are greater than 90° and that the bond angle between the two trans phosphines, $\text{P}(1)\text{--Ir--P}(2)$, is nonlinear (148.54(5)°). The positions of the hydride ligands were determined from difference Fourier maps, and these hydrides were allowed to refine isotropically. The observed Ir–H bond lengths (1.43(6) and 1.44(6) Å) are shorter than other such distances reported in the literature.³² This result is not unexpected due to the fact that X-ray analysis normally underestimates metal–hydrogen bond lengths in comparison to the more accurate distances determined by neutron diffraction.³³

(30) (a) Brunton, G. D.; Johnson, C. G. *J. Chem. Phys.* **1975**, *62*, 3797–3806. (b) Lundgren, J. O.; Tellgren, R. *Acta Crystallogr.* **1974**, *B30*, 1937.

(31) (a) Greenwood, N. N.; McDonald, W. S.; Reed, D.; Staves, J. *J. Chem. Soc., Dalton* **1979**, 1339. (b) Ferguson, G.; Hampden-Smith, M. J.; Dhubghaill, O. N.; Spalding, T. R. *Polyhedron* **1988**, *7*, 187. (c) Brown, J. M.; Evans, P. L.; Maddox, P. J.; Sutton, K. H. *J. Organomet. Chem.* **1989**, *359*, 115.

(32) In phosphine ligated, Ir(III)–hydride complexes, the Ir–H distances are often near 1.6 Å. (a) Eckert, J.; Jensen, C. M.; Koetzle, T. F.; Husebo, T. L.; Nicol, J.; Wu, P. *J. Am. Chem. Soc.* **1995**, *117*, 7271. (b) Bau, R.; Schwerdtfeger, C. J.; Garlaschelli, L.; Koetzle, T. F. *J. Chem. Soc., Dalton Trans.* **1993**, 3359. (c) Robertson, G. B.; Tucker, P. A. *Aust. J. Chem.* **1988**, *41*, 641.

(33) An example of the fact that M–H bond lengths may vary upon the use of either X-ray or neutron diffraction is illustrated in the following references. (a) Brammer, L.; Klooster, W. T.; Lemke, F. R. *Organometallics* **1996**, *15*, 1721–1727. (b) Brammer, L.; Lemke, F. R. *Organometallics* **1995**, *14*, 3980–3987.

(28) Meakin, P.; Muetterties, E. L.; Jesson, J. P. *J. Am. Chem. Soc.* **1973**, *95*, 75.2930.

(29) (a) Behr, A.; Herdtweck, E.; Herrmann, W. A.; Keim, W.; Kipshagen, W. *J. Chem. Soc., Chem. Commun.* **1986**, 1262. (b) Behr, A.; Herdtweck, E.; Herrmann, W. A.; Keim, W.; Kipshagen, W. *Organometallics* **1987**, *6*, 2307.

The average Ir–P bond distance is 2.3135(14) Å, slightly shorter than the corresponding distance of other $[\text{IrP}_4\text{H}_2]^{n+}$ complexes (2.341 Å).³¹ As with compound **3**, this shortening is attributed to the small cone angle and electronic nature of PTA. A strong trans influence is observed upon comparison of the Ir–P bond lengths that are trans to the hydride ligands (2.3382(14) Å) with those that are trans to the phosphines (2.2888(13) Å). The lengthening of a metal–ligand bond trans to a hydride is well established and observed in other $[\text{IrP}_4\text{H}_2]^{n+}$ compounds.^{29,31}

Reactivity of $[\text{Ir}(\text{PTA})_4(\text{CO})\text{Cl}]$ (3**).** Because of the interesting reactivity of $[\text{Ir}(\text{PTA})_3(\text{CO})\text{Cl}]$ (**1**) with HCl, we decided to investigate the same reaction with $[\text{Ir}(\text{PTA})_4(\text{CO})\text{Cl}]$ (**3**). As was seen with compound **1**, dissolution of **3** in 0.1 M HCl followed by slow diffusion of acetone results in the isolation of crystalline $[\text{Ir}(\text{PTAH})_2(\text{PTA})_2\text{Cl}_2]\text{Cl}_3$ (**4**) and $[\text{Ir}(\text{PTAH})_4(\text{H}_2)]\text{Cl}_5$ (**5**). Because of the extra PTA ligand of **3**, the yields of this process are greater than those of the reaction involving the trisphosphine complex, $[\text{Ir}(\text{PTA})_3(\text{CO})\text{Cl}]$ (**1**).

Discussion

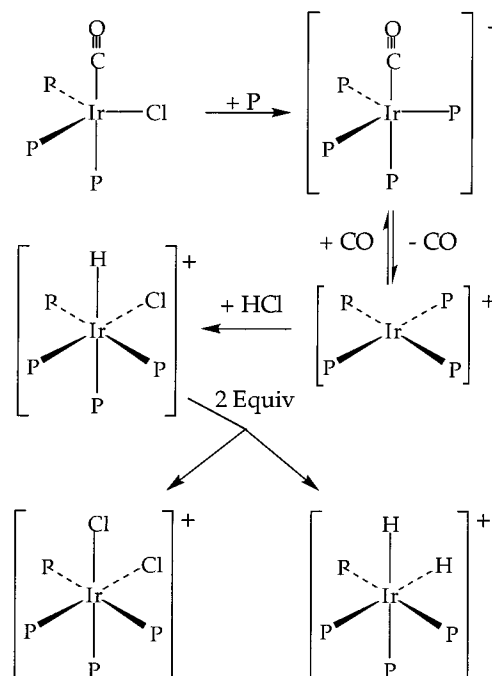
Unlike previously studied phosphine substitution reactions involving *trans*- $\text{Ir}(\text{CO})(\text{PPh}_3)_2\text{Cl}$,^{8c,34} the reaction of PTA with Vaska's compound does not form a PTA analogue thereof. Instead, the complexes $[\text{Ir}(\text{PTA})_3(\text{CO})\text{Cl}]$ (**1**) and $[\text{Ir}(\text{PTA})_4(\text{CO})\text{Cl}]$ (**3**) are prepared in good yields in absolute and 95% ethanol, respectively. Similar reactivity has been observed with the sterically less encumbering phosphine PMe_3 .²⁴ Therefore, it is undoubtedly the small cone angle of PTA (103°) that facilitates the formation of these tris and tetrakis phosphine complexes.

As evidenced by the X-ray structure of $[\text{Ir}(\text{PTA})_4(\text{CO})\text{Cl}]$ (**3**), the small cone angle also allows PTA to effectively coordinate to the metal center. This structure and the spectroscopic data of **1** and **3** indicate that optimal PTA ligation occurs at the equatorial sites, thus resigning the CO ligand to an axial position. This unique coordination makes the carbonyl labile as evidenced by the reactivity of **1** and **3**. Upon dissolution of **1** or **3** in dilute HCl, the CO is displaced to form a mixture of the dichloro species, $[\text{Ir}(\text{PTAH})_2(\text{PTA})_2\text{Cl}_2]\text{Cl}_3$ (**4**), and the dihydrido species, $[\text{Ir}(\text{PTAH})_4(\text{H}_2)]\text{Cl}_5$ (**5**).

This reactivity may be explained via the following mechanism (Scheme 2). In solution, $[\text{Ir}(\text{PTA})_3(\text{CO})\text{Cl}]$ (**1**) is in equilibrium with $[\text{Ir}(\text{PTA})_2(\text{CO})\text{Cl}]$ (**2**) and $[\text{Ir}(\text{PTA})_3(\text{CO})\text{Cl}]$. The free phosphine present in the equilibrium between **1** and **2** reacts with the 16-electron carbonyl, $[\text{Ir}(\text{PTA})_3(\text{CO})\text{Cl}]$, to form $[\text{Ir}(\text{PTA})_4(\text{CO})\text{Cl}]$ (**3**). Because of the weak, axial coordination of CO, the carbonyl is labile, and **3** is in equilibrium with the tetraphosphino, 16-electron Ir(I) complex $[\text{Ir}(\text{PTA})_4\text{Cl}]$. This reactive species oxidatively adds HCl to form the hydrido-chloro complex $[\text{Ir}(\text{PTA})_4(\text{H})(\text{Cl})\text{Cl}]$, the PEt_3 analog³⁵ of which has been crystallographically characterized. Isolation of equimolar concentrations of the dichloro complex, $[\text{Ir}(\text{PTAH})_2(\text{PTA})_2\text{Cl}_2]\text{Cl}_3$ (**4**), and the dihydrido compound, $[\text{Ir}(\text{PTAH})_4(\text{H}_2)]\text{Cl}_5$ (**5**), may be explained by invoking facile ligand exchange between 2 equiv of their hydrido-chloro precursor.

This mechanism is supported by the observation that, in absolute EtOH, $[\text{Ir}(\text{PTA})_4(\text{CO})\text{Cl}]$ (**3**) reacts with an ethereal

Scheme 2. Proposed Mechanism for the Production of **4** and **5**



solution of HCl to form a mixture of **4**, **5**, and the HCl complex ion, $[\text{Ir}(\text{PTA})_4(\text{H})(\text{Cl})\text{Cl}]^+$ (**6**). ^1H and $^{31}\text{P}\{^1\text{H}\}$ NMR analysis of this mixture indicated that, over a 3-day period, the concentrations of **4** and **5** increased while that of **6** decreased to zero. Even though we have been unable to isolate **6** as a pure compound, its identity was able to be determined upon comparison of its IR spectrum with those of other $[\text{IrP}_4(\text{H})(\text{L})]^{n+}$ complexes and its ^1H and ^{31}P NMR spectra with those of $[\text{Ir}(\text{PEt}_3)_4(\text{H})(\text{Cl})]^+$.³⁵ The $^{31}\text{P}\{^1\text{H}\}$ NMR spectrum (CD_2Cl_2 , 20 °C) of $[\text{Ir}(\text{PEt}_3)_4(\text{H})(\text{Cl})]^+$ contains a doublet of triplets (δ 27.3, int = 1, $^2J_{\text{P-P}_{\text{cis}}} = 14.2$ Hz, $^2J_{\text{P-P}_{\text{cis}}} = 12.1$ Hz), a triplet (δ 29.9, int = 2, $^2J_{\text{P-P}_{\text{cis}}} = 14.2$ Hz), and a multiplet (δ 37.0, int = 1, $^2J_{\text{P-P}_{\text{cis}}} = 14.2$ Hz, $^2J_{\text{P-P}_{\text{cis}}} = 12.1$ Hz). Because of the electronic differences between PTA and PEt_3 , the $^{31}\text{P}\{^1\text{H}\}$ frequencies assigned to the new complex are very different from this. Nevertheless, the presence of a doublet of triplets (δ -65.7, $^2J_{\text{P-P}_{\text{cis}}} = 18.6$ Hz, $^2J_{\text{P-P}_{\text{cis}}} = 16.7$ Hz), a triplet (δ -83.5, $^2J_{\text{P-P}_{\text{cis}}} = 18.6$ Hz), and a broad triplet (δ -91.7, $^2J_{\text{P-P}_{\text{cis}}} = 18.6$ Hz) in a 1:2:1 ratio still indicates that **6** is an octahedral species in which all but two cis coordination sites are occupied by phosphine. The IR spectrum of **6** contains an Ir–H stretch at 2075 cm^{-1} , indicating that one of the two remaining sites is occupied by a hydride ligand. This assignment is confirmed by the facts that similar frequencies have been observed for other $[\text{IrP}_4(\text{H})(\text{L})]^{n+}$ systems³⁶ and that the hydride region of the ^1H NMR spectrum contains a doublet of quartets (δ -12.00, $^2J_{\text{H-P}_{\text{trans}}} = 139$ Hz, $^2J_{\text{H-P}_{\text{cis}}} = 19$ Hz). A doublet of quartets (δ -13.24, $^2J_{\text{H-P}_{\text{trans}}} = 140$ Hz, $^2J_{\text{H-P}_{\text{cis}}} = 18$ Hz) is also present in the hydride region of the ^1H NMR spectrum of $[\text{Ir}(\text{PEt}_3)_4(\text{H})(\text{Cl})]^+$.³⁵

This study has shown that water is not an innocuous solvent toward complexes that are soluble in aqueous media. The thermodynamics of ligand hydration greatly affect the stability and reactivity of such metal compounds as indicated by the synthesis of $[\text{Ir}(\text{PTA})_3(\text{CO})\text{Cl}]$ (**1**) and its conversion into

(34) (a) Collman, J. P.; Kang, J. W. *J. Am. Chem. Soc.* **1967**, *89*, 844. (b) Smith, L. R.; Lin, S. M.; Chen, M. G.; Mondal, J. U. *Inorg. Synth.* **1982**, *21*, 97.

(35) Glegg, W.; Elsegood, M. R. J.; Scott, A. J.; Marder, T. B.; Dai, C.; Norman, N. C.; Pickett, N. L.; Robins, E. G. *Acta Crystallogr. C* **1999**, *55*, 733.

(36) (a) Milstein, D.; Calabrese, J. C.; Williams, I. D. *J. Am. Chem. Soc.* **1986**, *108*, 6387. (b) Thorn, D. L.; Tulip, T. H. *Organometallics* **1982**, *1*, 1580.

$[\text{Ir}(\text{PTA})_4(\text{CO})]\text{Cl}$ (**3**). This study has also shown that the use of water as a medium for organometallic reactions is complex and possibly misleading. As was observed for the synthesis of $[\text{Ir}(\text{PTA})_4(\text{H})(\text{Cl})]^+$ (**6**), reactions of organometallic complexes with HCl in water may still be viewed as oxidative additions, even though water is well-known to activate hydrogen halides. An understanding of these and other processes is of great value for the study of water-soluble catalysis, and therefore the Ir–PTA complexes reported herein may serve as beneficial models for this endeavor. Ir–PTA compounds may also function as catalysts themselves. The lability of the carbonyl and the resistance of PTA to oxidation may allow **3** to serve as an effective carbonylation catalyst. The presence of two hydride ligands, along with the aqueous and acidic stability of **5**, may allow it to function as a water-soluble hydrogenation catalyst.

Experiments are presently being performed to explore these and other possibilities.

Acknowledgment. Acknowledgment is made to the donors of the Petroleum Research Fund, administered by the American Chemical Society, for partial support (Grant 33818-GB3 to D.A.K. and Grant 33450-GB3 to J.A.H.) of this research. We would also like to acknowledge and thank Dr. Steve Philson and Dr. Letitia Yao at the University of Minnesota for their assistance with the ^{31}P NMR spectral analyses.

Supporting Information Available: X-ray crystallographic files in CIF format for complexes **3** and **5** ($[\text{Ir}(\text{PTA})_4(\text{CO})]\text{Cl}$ and $[\text{Ir}(\text{PTAH})_3(\text{PTAH}_2)(\text{H})_2]\text{Cl}_6$). This material is available free of charge via the Internet at <http://pubs.acs.org>.

IC000501L